THE INFLUENCE OF GEOMETRY OF THE SPECIMEN AND MATERIAL PROPERTIES ON THE Q-STRESS VALUE NEAR THE CRACK TIP FOR SEN(T) SPECIMEN

Marcin GRABA*

*Kielce University of Technology, Faculty of Mechatronics and Machine Design,
Chair of Fundamentals of Machine Design, Al. 1000-lecia PP 7, 25-314 Kielce, Poland

mgraba@tu.kielce.pl

Abstract: In the paper the short theoretical backgrounds about elastic-plastic fracture mechanics were presented and the O'Dowd-Shih theory was discussed. Using ADINA System program, the values of the Q-stress determined for various elastic-plastic materials for SEN(T) specimen – single edge notched plates in tension – were presented. The influence of kind of the specimen, crack length and material properties (work-hardening exponent and yield stress) on the Q-parameter were tested. The numerical results were approximated by the closed form formulas. Presented in the paper results are complementary of the two papers published in 2007 (Graba, 2007) and in 2010 (Graba, 2010), which show and describe influence of the material properties and crack length for the Q-stress value for SEN(B) and CC(T) specimens respectively. Presented and mentioned papers show such catalogue of the Q-stress value, which may be used in engineering analysis for calculation of the real fracture toughness.

1. INTRODUCTION TO ELASTIC-PLASTIC FRACTURE MECHANICS

In 1968 J. W. Hutchinson (ADINA 8.4.1, 2006a) published the fundamental paper, which characterized stress fields in front of a crack for non-linear Ramberg-Osgood (R-O) material in the form:

$$\sigma_{ij} = \sigma_0 \left(\frac{J}{\alpha \sigma_0 \varepsilon_0 I_n r} \right)^{\frac{1}{1+n}} \tilde{\sigma}_{ij}(\theta, n) \tag{1}$$

where r and θ are polar coordinates of the coordinate system located at the crack tip, σ_{ij} are the components of the stress tensor, J is the *J*-integral, n is R-O exponent, α is R-O constant, σ_0 is yield stress, ε_0 is strain related to σ_0 through $\varepsilon_0 = \sigma_0/E$. Functions $\tilde{\sigma}_{ij}(n,\theta)$, $I_n(n)$ must be found by solving the fourth order non-linear homogenous differential equation independently for plane stress and plane strain (Hutchinson, 1968). Equation (1) is commonly called the "HRR solution" (Fig. 1).

The HRR solution includes the first term of the infinite series only. The numerical analysis shown, that results obtained using the HRR solution are different from the results obtained using the finite element method (FEM) - see Fig. 2. To eliminate this difference, it's necessary to use more terms in the HRR solution.

In 1985 Li and et. (Li and Wang, 1985) proposed the another stress field description, which was used two terms in the Airy function. They obtained the second term of the asymptotic expansion for the two materials described by two different work-hardening exponent: n=3 and n=10. Next, they compared their results with the HRR fields and FEM results. Their analysis shown, that using the two term solution to describe the stress field near the crack tip, brings closer analytical results to FEM results. Two term solution much better describes the stress field near the crack tip, and the value of the second term, which may not to be negligible depends on the material properties and the geometry specimen.

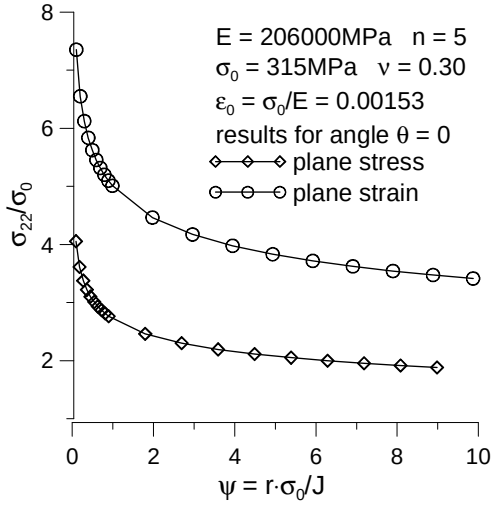

Fig. 1. The crack opening stress distribution for elastic-plastic materials, obtained using the HRR solution

In 1993 Yang and et. (Yang et al., 1993) using the Airy function with the separate variables in the infinite series form, proposed, that stress field near the crack tip may be described by the Eq. (2) in the infinite series form:

$$\frac{\sigma_{ij}}{\sigma_0} = \sum_{k=1}^{+\infty} A_k \bar{r}^{s_k} \tilde{\sigma}_{ij}^{(k)}(\theta) \tag{2}$$

where k is the number of the series terms, A_k is the amplitude for the k series term, $\bar{r}$ is the normalized distance from the crack tip, s_k is power exponent for the k series term, and $\tilde{\sigma}_{ij}^{(k)}$ is "stress" function.

Using only three terms of the infinite series, Eq. (2) may be written in the following form:

$$\frac{\sigma_{ij}}{\sigma_0} = A_1 \bar{r}^{\,s} \tilde{\sigma}_{ij}^{(1)}(\theta) + A_2 \bar{r}^{\,t} \tilde{\sigma}_{ij}^{(2)}(\theta) + \frac{A_2^2}{A_1} \bar{r}^{\,2t-s} \tilde{\sigma}_{ij}^{(3)}(\theta) \qquad (3)$$

where the $\tilde{\sigma}_{ij}^{(k)}$ functions must be found by solving the fourth order non-linear homogenous differential equation independently for plane stress and plane strain, s is the power exponent, which is identical to the one in the HRR solution (s may be calculated as s=-1/(n+1)), t is the power exponent for the second term of the asymptotic expansion, which must be found numerically by solving the fourth order non-linear homogenous differential equation independently for plane stress and plane strain, $\bar{r}$ is the normalized distance from the crack tip calculated as $\bar{r} = r/(J/\sigma_0)$, A_1 is the amplitude of the first term of the infinite series evaluated as $A_1 = (\alpha \varepsilon_0 I_n)^{-1/(n+1)}$, and A_2 is the amplitude of the second term, which is calculated by fitting the Eq. (3) to the numerical results of the stress fields close to crack tip.

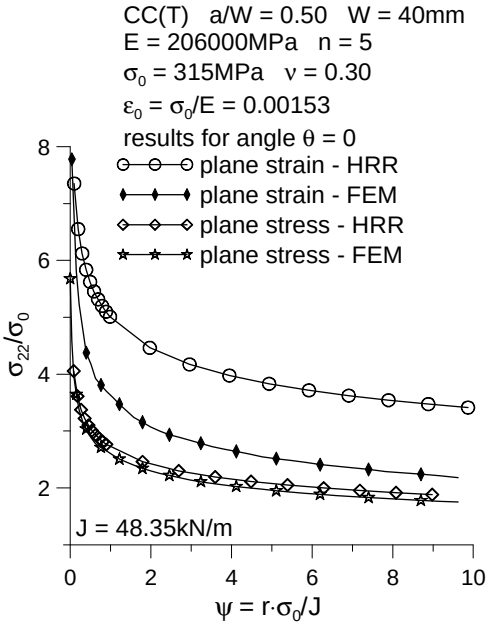

Fig. 2. Comparison the FEM results and HRR solution for plane stress and plane strain for center cracked plate in tension (CC(T))

In 1993 Shih et al. (1993) proposed simplified solution. They assumed, that the FEM results are exact and computed the difference between the numerical and HRR results. They proposed, that the stress field near the crack tip, may be described using only two terms, by following equation:

$$\frac{\sigma_{ij}}{\sigma_0} = \left(\frac{J}{\alpha \varepsilon_0 \sigma_0 I_n r} \right)^{1/(n+1)} \tilde{\sigma}_{ij}(\theta; n) + Q \left(\frac{r}{J/\sigma_0} \right)^{q} \hat{\sigma}_{ij}(\theta; n) \qquad (4)$$

where $\hat{\sigma}_{ij}(\theta, n)$ are functions evaluated numerically, q is the power exponent, which value changes in the range (0; 0.071), and Q is the parameter, which is the amplitude of the second term asymptotic solution. The Q-parameter is commonly called the "Q-stress".

O'Dowd and Shih (1991, 1992), tested the Q-parameter in the range J/σ_0<r<5J/σ_0 near the crack tip. They showed, that the Q-parameter weakly depend on crack tip distance in the range of the ±π/2 angle. O'Dowd and Shih proposed only two terms to describe the stress field near the crack tip:

$$\sigma_{ij} = (\sigma_{ij})_{HRR} + Q \sigma_0 \hat{\sigma}_{ij}(\theta) \qquad (5)$$

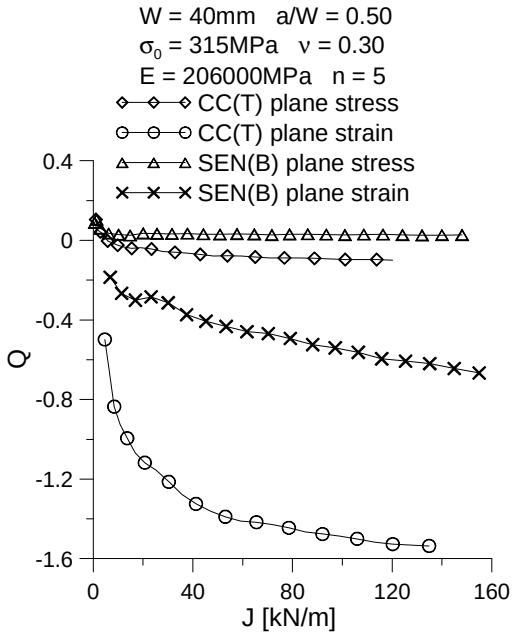

Fig. 3. The comparison of the J-Q trajectories for CC(T) and SEN(B)

To avoid the ambiguity during the calculation of the Q-stress, O'Dowd and Shih (O'Dowd, Shih, 1991), (O'Dowd, Shih, 1992) have suggested, where the Q-stress may be evaluated. It was assumed, that the Q-stress should be computed at distance from crack tip, which is equal to r=2J/σ_0 for θ=0 direction. O'Dowd and Shih postulated, that for θ=0 the function $\hat{\sigma}_{\theta\theta}(\theta = 0)$ is equal to 1. That's why, the Q-stress may be calculated from following relationship:

$$Q = \frac{(\sigma_{\theta\theta})_{FEM} - (\sigma_{\theta\theta})_{HRR}}{\sigma_0} \text{ for } \theta=0 \text{ and } \frac{r\sigma_0}{J} = 2 \qquad (6)$$

where $(\sigma_{\theta\theta})_{FEM}$ is the stress value calculated using FEM and $(\sigma_{\theta\theta})_{HRR}$ is stress value evaluated form HRR solution. During analysis, O'Dowd and Shih shown, that in the range of θ=±π/4, the following relationships take place: $Q\hat{\sigma}_{\theta\theta} \approx Q\hat{\sigma}_{rr}$, $\hat{\sigma}_{\theta\theta}/\hat{\sigma}_{rr} \approx 1$ and $Q\hat{\sigma}_{r\theta} \approx 0$ (because $Q\hat{\sigma}_{r\theta} << Q\hat{\sigma}_{\theta\theta}$). Thus, the Q-stress value determines the level of the hydrostatic stress. For plane stress, the Q-parameter is equal to zero, but for plane strain, the Q- parameter is in the most cases smaller than zero (Fig. 3).

2. DISCUSSION ABOUT ENGINEERING APPLICATIONS OF THE *J-Q* THEORY

To describe the stress field near the crack tip for elastic-plastic materials, the HRR solution is most often used (Eq. 1). However the results obtained are usually overesti-

mated and analysis is conservative. The HRR solution includes the first term of the infinite series only.

The numerical analysis shown, that results obtained using the HRR solution are different from the results obtained using the finite element method (FEM) – see Fig. 2. To eliminate this difference, it's necessary to use more terms in the HRR solution, for example the J-A_2 theory suggested by Yang and et. (Yang et al., 1993), or the O'Dowd and Shih approach – the J-Q theory (O'Dowd, and Shih, 1991).

For using the O'Dowd approach, engineer needs only the Q-stress distribution, which must be calculated numerically. That's why O'Dowd approach is easier and pleasanter in use in contrast to J-A_2 theory. Using the J-A_2 theory proposed by Yang and el., first engineer must solve fourth order nonlinear differential equation to determine the $\tilde{\sigma}_{ij}^{(k)}$ function and the t power exponent. Next, the engineer using FEM results calculated the A_2 amplitude by fitting the Eq. 3 to numerical results.

The J-Q theory found application in European Engineering Programs, like SINTAP (Sintap, 1999) or FITNET (Fitnet, 2006). The Q-stress are applied under construction the fracture criterion and to assessment the fracture toughness of the structural component. Thus O'Dowd theory has practical application in engineering issues.

Sometimes using the J-Q theory may be limited, because there is no value of the Q-stress for given material and specimen. Using any fracture criterion, for example proposed by O'Dowd (O'Dowd, 1995), or another criterion, the engineer can estimate fracture toughness quit a fast, if the Q-stress are known. Literature doesn't announce the Q-stress catalogue and Q-stress value as function of external load, material properties or geometry of the specimen. In some articles, the engineer may find the J-Q graphs for certain group of material.

The best solution will be, origin the catalogue of the J-Q graphs for materials characterized by various yield strength, different work-hardening exponent. Such catalogue should take into consideration the influence of the external load, kind of the specimen (SEN(B) specimen – bending, SEN(T) specimen – tension) and geometry of the specimen, too. For SEN(B) and CC(T) specimens, such catalogues were presented by Graba in 2007 (Graba, 2007) and in and 2010 (Graba, 2010) respectively.

In the next parts of the paper, the values of the Q-stress will be determined for various elastic-plastic materials for single edge notched specimens in tension (SEN(T)). The SEN(T) specimen is the basic structural element, which is used in the FITNET procedures to modeling real constructions. All results will be approximated by the closed form formulas.

3. DETAILS OF NUMERICAL ANALYSIS

In the numerical analysis, the single edge notched specimens in tension (SEN(T)) were used (Fig. 4). Dimensions of the specimens satisfy the standard requirement which is set up in FEM calculation - $L \geq 2W$, where W is the width of the specimen and L is the measuring length of the specimen. Computations were performed for plane strain using small strain option. The relative crack length was equal to a/W={0.20, 0.50, 0.70} where a is a crack length and the width of specimens W was equal to 40mm. For this case, the measuring length L satisfied the condition $L \geq 80$mm.

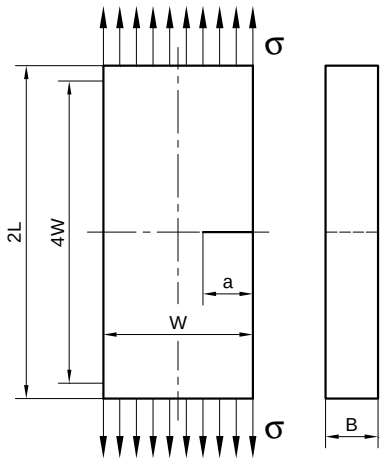

Fig. 4. The single edge notched specimen in tension (SEN(T)) used in the numerical analysis

The choice of the SEN(T) specimen was intentional, because the SEN(T) specimens are used in the FITNET procedures to modeling real structural elements. Also in FITNET procedures, the limit load and stress intensity factors solutions for SEN(T) specimens are presented. However in the EPRI procedures (Kumar et al., 1981), the hybrid method for calculation the J-integral is given. Also some laboratory test in order to determine the critical values of the J-integral, may be done using the SEN(T) specimen.

Computations were performed using ADINA SYSTEM 8.4 (Adina, 2006a, b). Due to the symmetry, only a half of the specimen was modeled. The finite element mesh was filled with the 9-node plane strain elements with nine (3×3) Gauss integration points. The size of the finite elements in the radial direction was decreasing towards the crack tip, while in the angular direction the size of each element was kept constant. The crack tip region was modeled using 50 semicircles. The first of them, was at least 20 times smaller then the last one. It also means, that the first finite element behind to crack tip is smaller 2000 times than the width of the specimen. The crack tip was modeled as quarter of the arc which radius was equal to $r_w=1\cdot10^{-6}$m (it's $(0.000025\times W)$. The whole SEN(T) specimen was modeled using 323 finite elements and 1353 nodes. External load was applied to bottom edge of the specimen. The example finite element model for SEN(T) specimen used in the numerical analysis is presented on Fig. 5.

In the FEM simulation, the deformation theory of plasticity and the von Misses yield criterion were adopted. In the model the stress–strain curve was approximated by the relation:

$$\frac{\varepsilon}{\varepsilon_0} = \begin{cases} \sigma/\sigma_0 & \text{for } \sigma \leq \sigma_0 \\ \alpha(\sigma/\sigma_0)^n & \text{for } \sigma > \sigma_0 \end{cases} \tag{7}$$

where α=1. The tensile properties for the materials which were used in the numerical analysis are presented below

in the Tab.1. In the FEM analysis, calculations were done for sixteen materials, which were differed by yield stress and the work hardening exponent.

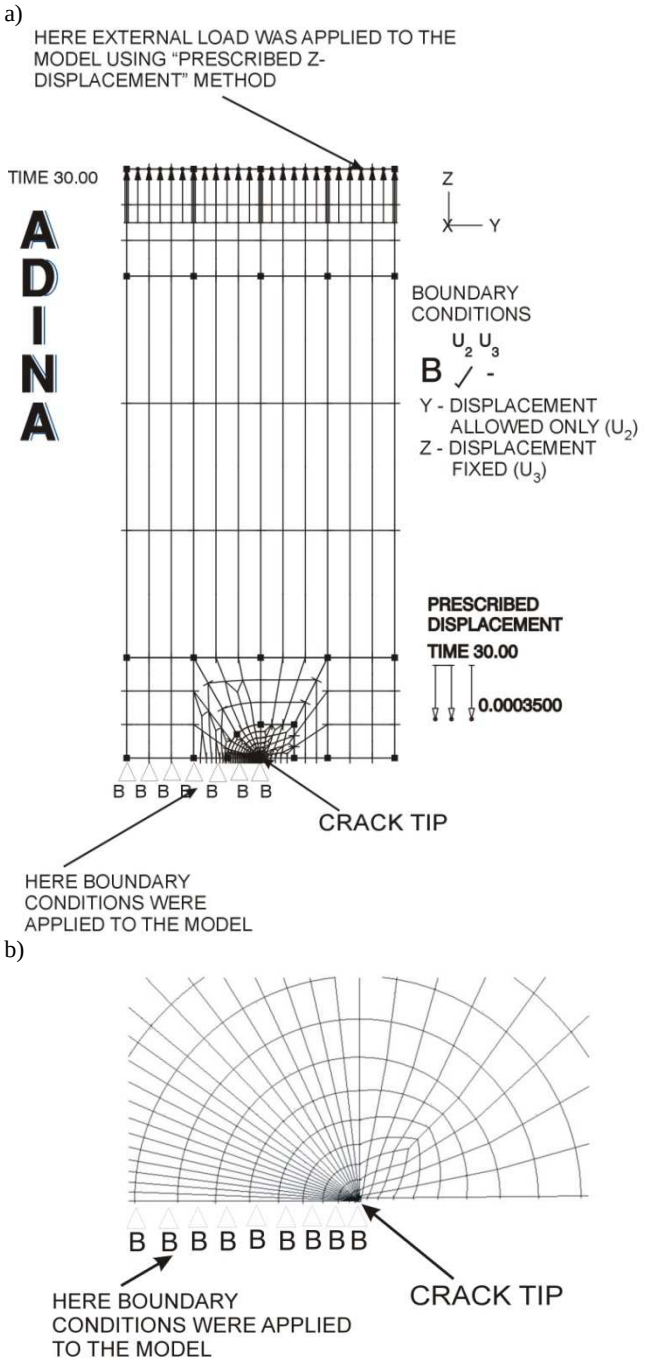

Fig. 5. a) The finite element model for SEN(T) specimen used in the numerical analysis; b) The finite elements mesh near crack tip using in the numerical analysis

Tab. 1. The mechanical properties of the materials used in numerical analysis and the HRR parameters for plane strain

σ_0 [MPa]	E [MPa]	ν	$\varepsilon_0=\sigma_0/E$	α	n	$\tilde{\sigma}_{\theta\theta}(\theta=0)$	I_n
315	206000	0.3	0.00153	1	3	1.94	5.51
500			0.00243		5	2.22	5.02
1000			0.00485		10	2.50	4.54
1500			0.00728		20	2.68	4.21

The J-integral were calculated using two methods. The first method, called the "virtual shift method", uses concept of the virtual crack growth to compute the virtual energy change. The second method is based on the J–integral definition:

$$J=\int_C \left[w dx_2 - \boldsymbol{t}(\partial \boldsymbol{u}/\partial x_1) ds\right] \tag{8}$$

where w is the strain energy density, $\boldsymbol{t}$ is the stress vector acting on the contour C drawn around the crack tip, $\boldsymbol{u}$ denotes displacement vector and ds is the infinitesimal segment of contour C.

In summary, in the numerical analysis 48 SEN(T) specimens were used, which were differed by crack length and material properties.

4. ANALYSIS OF THE NUMERICAL RESULTS

The analysis of the results obtained was made in the range $J/\sigma_0<r<6J/\sigma_0$ near the crack tip, and its shown, that the Q-stress decrease if the distance from the crack tip increase (Fig. 6). If the external load increases, the Q-stress decreases and the difference between Q-stress calculated in the following measurement points increase (Fig. 6). If the crack length decrease then Q-stress reaches more negative value for the same J-integral level (Fig. 7).

For the sake of the fact, that the Q-parameter, which is used in fracture criterion is calculated at distance equal to $r=2J/\sigma_0$, it's necessary to notice some comments about obtained results. If the yield stress increases, the Q-parameter increase too, and it reflects for all SEN(T) specimen with different crack length a/W (Fig. 8). For smaller yield stress the J-Q trajectories shape up well lower and it's observed faster changes of the Q-parameter if the external load is increase (Fig. 8).

For SEN(T) specimens, the ambiguous behavior of the J-Q trajectories depending of the work-hardening exponent is observed. For specimens with short cracks (a/W=0.20) and the same yield stress, for smaller values of the work-hardening exponent n (e.g. $n\leq5$), the Q-stress become less negative (Fig. 9). For specimens with the normative crack length (a/W=0.50) or with the long cracks (a/W=0.70), the cutting of the J-Q trajectories was observed (Fig. 10 and Fig. 11) - first the higher values of the Q-stress were observed for specimen characterized by strongly hardening material, but for increasing external load the reversal of the trend took place and the higher Q-stress were observed for specimens characterized by weakly hardening material.

For short cracks the Q-stress value drops more rapidly then for long ones in the range of the small external load (Fig. 7). For specimen with long cracks (a/W=0.70), the another nature of the J-Q trajectories was observed than for specimen with relative cracks length $a/W\leq0.50$ (Fig. 7). It may be a consequence of the absence in the analysis of the stress field, the consideration of the bending stress near the crack tip, which was discussed by Chao et al., (2004).

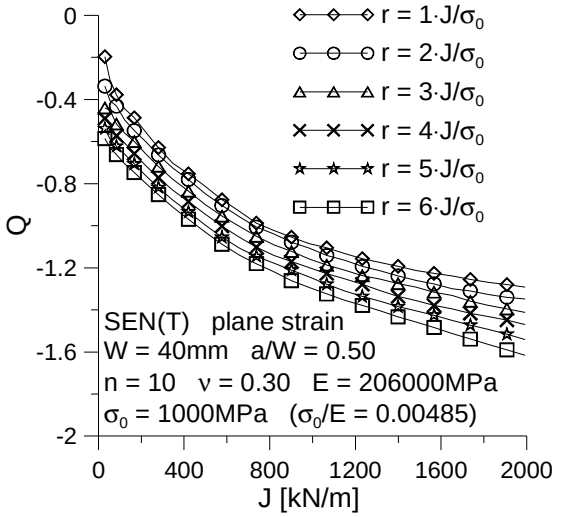

Fig. 6. "The *J-Q* family curves" for SEN(T) specimen calculated at six distances *r* from crack tip

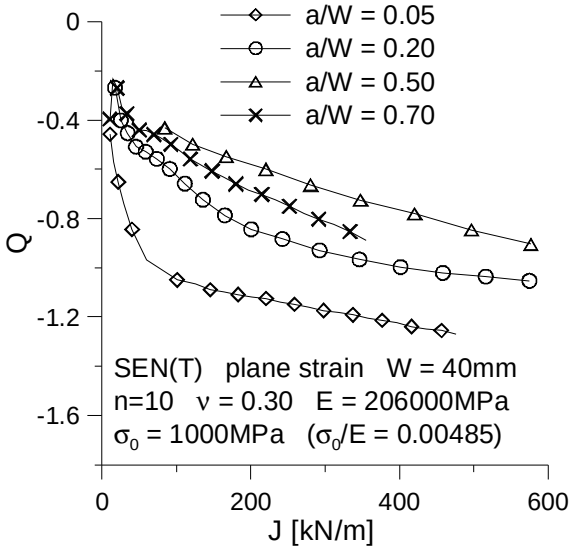

Fig. 7. The influence of the crack length on *J-Q* trajectories for SEN(T) specimens

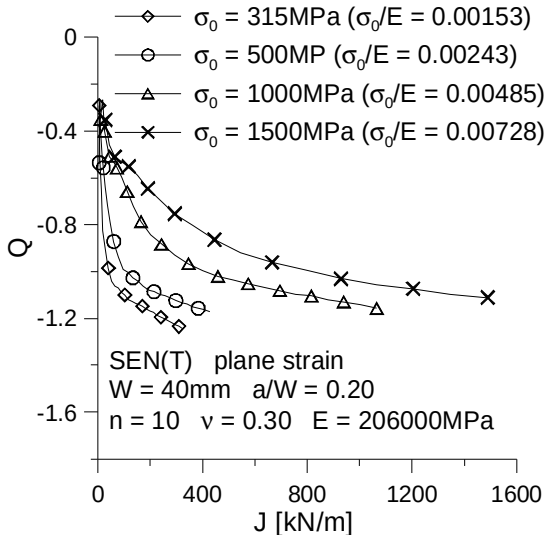

Fig. 8. The influence of the yield stress on *J-Q* trajectories for SEN(T)

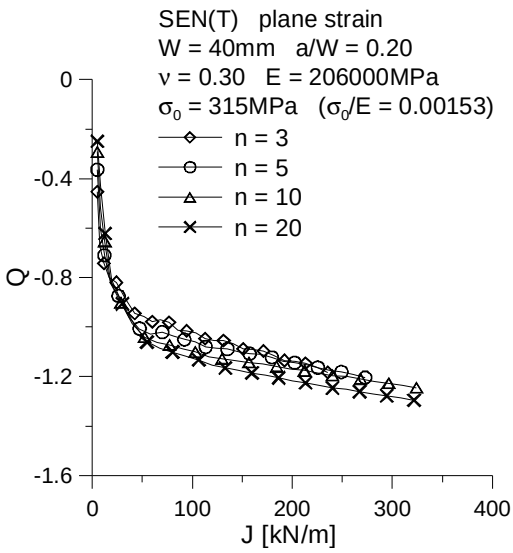

Fig. 9. The influence of the work hardening exponent on *J-Q* trajectories for SEN(T) specimens (a/W=0.20, σ_0=315MPa)

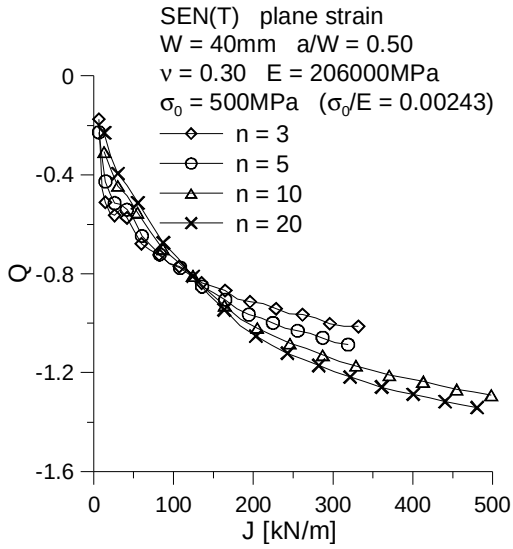

Fig. 10. The influence of the work hardening exponent on *J-Q* trajectories for SEN(T) specimens (a/W=0.50, σ_0=500MPa)

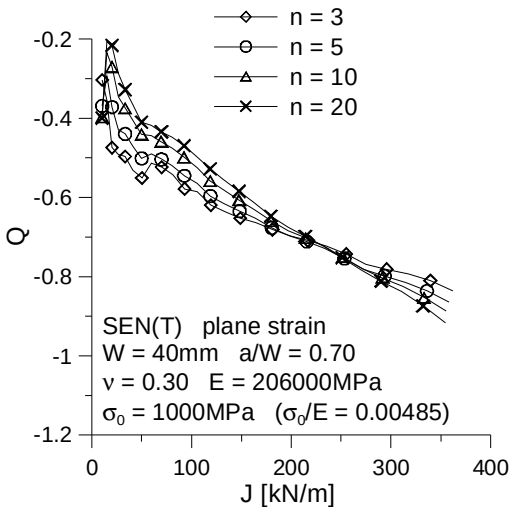

Fig. 11. The influence of the work hardening exponent on *J-Q* trajectories for SEN(T) specimens (a/W=0.70, σ_0=1000MPa)

5. APPROXIMATION OF THE NUMERICAL RESULTS

In the literature the mathematic formulas, to calculate the *Q*-stress taking into consideration the level of external load, material properties and geometry of the specimen are not known for the most of the cases. Presented in the paper numerical computations provided with the *J-Q* catalogue and the universal formula (9), which allows to calculate the *Q*-stress and take into consideration all the parameters influencing the value of the *Q*-stress. All results, were presented in the Q=f(log($J/(a\cdot\sigma_0)$)) graph forms. Next all graphs were approximated by the simple mathematical formulas, taking the material properties, external load and geometry specimen into consideration. All the approximations were made for results obtained at the distance $r=2.0\cdot J/\sigma_0$. Each of the obtained trajectories Q=f(log($J/(a\cdot\sigma_0)$)), was approximated by the third order polynomial in the form:

$$Q(J,a,\sigma_0)=A+B\cdot\left(\log\left(\frac{J}{(a\cdot\sigma_0)}\right)\right)+ +C\cdot\left(\log\left(\frac{J}{(a\cdot\sigma_0)}\right)\right)^2+D\cdot\left(\log\frac{J}{(a\cdot\sigma_0)}\right)^3 \quad (9)$$

where the *A*, *B*, *C*, *D* coefficients depend on the work-hardening exponent *n*, yield stress σ_0 and crack length *a*/*W*. The rank of the fitting the formula (9) to numerical results for the worst case was equal R^2=0.95. For different work hardening exponents *n*, yield stresses σ_0 and ratios *a*/*W*, which were not include in the numerical analysis, the coefficients *A*, *B*, *C* and *D* may be evaluated using the linear or quadratic approximation. Results of the approximation (all coefficients of the approximation numerical results by Eq. (9)) are presented in Tables 2-4.

Tab. 2. The coefficients of equation (9) for SEN(T) specimen with the crack length *a*/*W*=0.20

σ_0 = 315MPa			σ_0/E = 0.00153		
n	*A*	*B*	*C*	*D*	R^2
3	-2.476	-2.221	-1.165	-0.228	0.993
5	-2.128	-1.722	-0.999	-0.223	0.997
10	-1.752	-0.991	-0.604	-0.163	0.998
20	-1.677	-0.683	-0.379	-0.121	0.997
σ_0 = 500MPa			σ_0/E = 0.00243		
n	*A*	*B*	*C*	*D*	R^2
3	-1.618	-0.876	-0.397	-0.087	0.986
5	-1.105	0.104	0.119	-0.008	0.996
10	-1.365	-0.139	0.029	-0.026	0.996
20	-1.465	-0.145	0.075	-0.017	0.996
σ_0 = 1000MPa			σ_0/E = 0.00485		
n	*A*	*B*	*C*	*D*	R^2
3	-1.875	-1.438	-0.651	-0.119	0.958
5	-1.198	0.007	0.217	0.037	0.990
10	-1.065	0.552	0.622	0.116	0.995
20	-1.163	0.533	0.654	0.122	0.996
σ_0 = 1500MPa			σ_0/E = 0.00728		
n	*A*	*B*	*C*	*D*	R^2
3	-1.601	-1.099	-0.477	-0.089	0.982
5	-1.469	-0.537	-0.056	-0.002	0.990
10	-1.401	-0.078	0.328	0.080	0.996
20	-1.486	-0.085	0.364	0.088	0.996

Tab. 3. The coefficients of equation (9) for SEN(T) specimen with the crack length *a*/*W*=0.50

σ_0 = 315MPa			σ_0/E = 0.00153		
n	*A*	*B*	*C*	*D*	R^2
3	-2.743	-1.606	-0.456	-0.059	0.990
5	-2.909	-1.516	-0.334	-0.038	0.990
10	-0.621	1.913	1.291	0.205	0.996
20	0.238	3.364	2.03142	0.320	0.996
σ_0 = 500MPa			σ_0/E = 0.00243		
n	*A*	*B*	*C*	*D*	R^2
3	-3.927	-3.615	-1.435	-0.209	0.982
5	-3.383	-2.414	-0.728	-0.088	0.995
10	-2.009	-0.132	0.435	0.094	0.997
20	-1.810	0.450	0.811	0.160	0.997
σ_0 = 1000MPa			σ_0/E = 0.00485		
n	*A*	*B*	*C*	*D*	R^2
3	-4.009	-4.031	-1.629	-0.229	0.977
5	-2.662	-1.869	-0.545	-0.059	0.997
10	-2.773	-1.760	-0.403	-0.032	0.996
20	-2.971	-1.789	-0.312	-0.006	0.997
σ_0 = 1500MPa			σ_0/E = 0.00728		
n	*A*	*B*	*C*	*D*	R^2
3	-2.612	-2.335	-0.943	-0.138	0.994
5	-2.505	-1.895	-0.629	-0.078	0.999
10	-2.559	-1.688	-0.420	-0.035	0.996
20	-2.357	-1.041	0.048	0.059	0.997

Fig. 12 presents the comparison of the numerical results and their approximation for *J-Q* trajectories for several cases of the SEN(T) specimens. Fig.s 13-15 presents in the graphical form some numerical results obtained for SEN(T) specimens in plain strain. All results are presented using the *J-Q* trajectories.

Tab. 4. The coefficients of equation (9) for SEN(T) specimen with the crack length *a*/*W*=0.70

σ_0 = 315MPa			σ_0/E = 0.00153		
n	*A*	*B*	*C*	*D*	R^2
3	-6.051	-4.762	-1.512	-0.179	0.989
5	-3.287	-0.872	0.171	0.049	0.991
10	0.290	3.710	2.045	0.294	0.993
20	4.424	8.931	4.175	0.574	0.993
σ_0 = 500MPa			σ_0/E = 0.00243		
n	*A*	*B*	*C*	*D*	R^2
3	-8.575	-8.072	-2.818	-0.341	0.989
5	-10.470	-9.908	-3.417	-0.410	0.997
10	-11.036	-9.958	-3.227	-0.365	0.998
20	-0.753	2.846	1.979	0.325	0.993
σ_0 = 1000MPa			σ_0/E = 0.00485		
n	*A*	*B*	*C*	*D*	R^2
3	-6.703	-6.471	-2.323	-0.286	0.985
5	-7.237	-6.937	-2.456	-0.301	0.996
10	-7.642	-7.198	-2.481	-0.297	0.998
20	-8.527	-8.058	-2.747	-0.325	0.997
σ_0 = 1500MPa			σ_0/E = 0.00728		
n	*A*	*B*	*C*	*D*	R^2
3	-5.580	-5.462	-2.021	-0.256	0.976
5	-5.819	-5.576	-2.011	-0.250	0.995
10	-5.990	-5.608	-1.961	-0.238	0.998
20	-7.453	-7.315	-2.617	-0.322	0.999

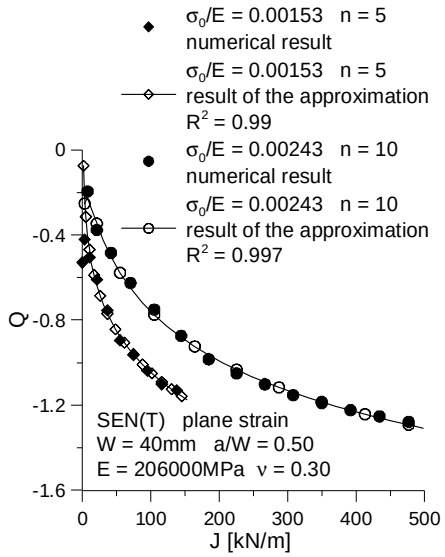

Fig. 12. Comparison of the numerical results and their approximation for *J*-*Q* trajectories for SEN(T) specimens with relative crack length a/W=0.50: σ_0={315, 500}MPa, n={5, 10}

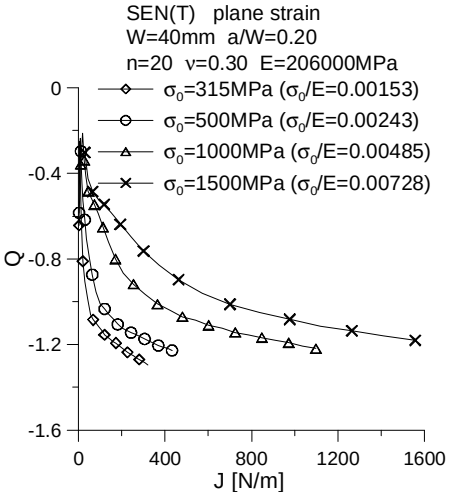

Fig. 13. Sample numerical results obtained for SEN(T) specimens: the influence of the yield stress on *J*-*Q* trajectories for specimens with crack length a/W=0.20 and for power exponents n=20

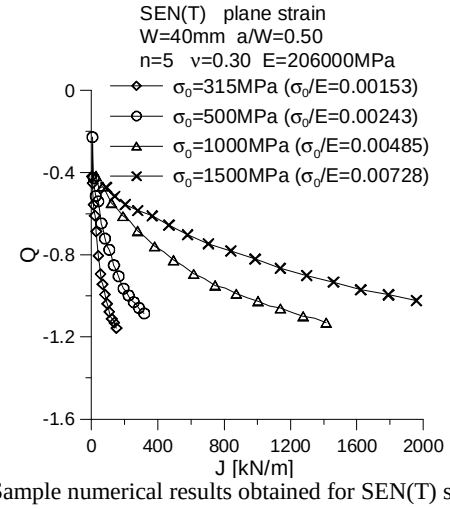

Fig. 14. Sample numerical results obtained for SEN(T) specimens: the influence of the yield stress on *J*-*Q* trajectories for specimens with crack length a/W=0.50 and for power exponents n=5

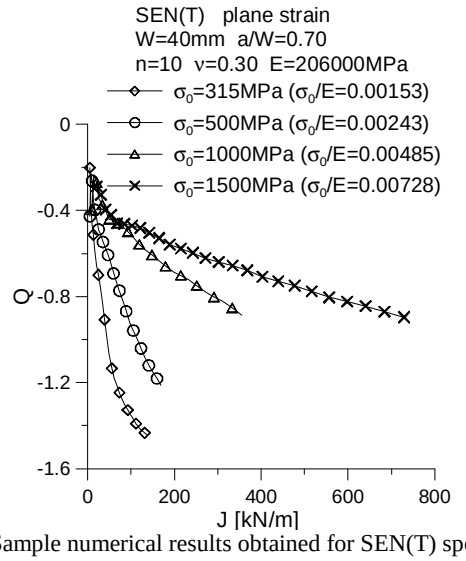

Fig. 15. Sample numerical results obtained for SEN(T) specimens: the influence of the yield stress on *J*-*Q* trajectories for specimens with crack length a/W=0.70 and for power exponents n=10

6. SUMMARY

In the paper the values of the Q-stress were determined for various elastic-plastic materials for single edge notched specimens in tension (SEN(T)). The influence of the yield strength, the work-hardening exponent and the crack length on the *Q*-parameter was tested. The numerical results were approximated by the closed form formulas. The most important results are summarized as follows:

- the *Q*-stress depends on geometry and external the load; different values of the *Q*-stress are obtained for center cracked plane in tension (CC(T)) and different for the SEN(T) specimen, which are characterized by the same material properties;
- the *Q*-parameter is a function of the material properties; its value depends on the work-hardening exponent n and the yield stress σ_0;
- if the crack length decrease then *Q*-stress reaches more negative value for the external load.

REFERENCES

1. **ADINA 8.4.1** (2006a), ADINA: User Interface Command Reference Manual - Volume I: ADINA Solids & Structures Model Definition, *Report ARD 06-2*, ADINA R&D, Inc.
2. **ADINA 8.4.1** (2006b), ADINA: Theory and Modeling Guide - Volume I: ADINA, *Report ARD 06-7*, ADINA R&D, Inc.
3. **FITNET** (2006), FITNET Report, (European Fitness-for-service Network), Edited by M. Kocak, S. Webster, J. J. Janosch, R. A.Ainsworth, R.Koers, *Contract No. G1RT-CT-2001-05071*.
4. **Graba M**. (2007)**,** Wpływ stałych materiałowych na rozkład naprężeń Q przed wierzchołkiem pęknięcia w materiałach sprężysto - plastycznych, *IV MSMZMiK - Augustów 2007*, materiały konferencyjne, 109-114;
5. **Graba M**. (2010)**,** Wpływ stałych materiałowych na rozkład naprężeń *Q* przed wierzchołkiem pęknięcia w materiałach sprężysto-plastycznych dla płyty z centralną szczeliną poddanej rozciąganiu, *Acta Mechanica et Automatica*, Vol. 4, No. 2, 54-62.

6. **Hutchinson J. W.** (1968), Singular Behaviour at the End of a Tensile Crack in a Hardening Material, *Journal of the Mechanics and Physics of Solids*, 16, 13-31.
7. **Kumar V., German M. D., Shih C. F.** (1981), An Engineering Approach for Elastic-Plastic Fracture Analysis, *EPRI Report* NP-1931, Electric Power Research Institute, Palo Alto, CA., 1981.
8. **Li Y., Wang Z.** (1985), High-Order Asymptotic Field of Tensile Plane-Strain Nonlinear Crack Problems, *Scientia Sinica (Series A)*, Vol. XXIX, No. 9, 941-955.
9. **O'Dowd N. P.** (1995), Applications of two parameter approaches in elastic-plastic fracture mechanics, *Engineering Fracture Mechanics*, Vol. 52, No. 3, 445-465.
10. **O'Dowd N. P., Shih C. F.** (1991), Family of Crack-Tip Fields Characterized by a Triaxiality Parameter – I. Structure of Fields, *J. Mech. Phys. Solids*, Vol. 39, No. 8, -1015.
11. **O'Dowd N. P., Shih C. F.** (1992), Family of Crack-Tip Fields Characterized by a Triaxiality Parameter – II. Fracture Applications, J. *Mech. Phys. Solids*, Vol. 40, No. 5, 939-963.
12. **Shih C. F., O'Dowd N. P., Kirk M. T.** (1993), A Framework for Quantifying Crack Tip Constraint, *Constraint Effects in Fracture*, ASTM STP 1171, E.M. Hackett, K,-H. Schwalbe, R. H. Dodds, Eds., American Society for Testing and Materials, Philadelphia, 2-20.
13. **SINTAP** (1999), SINTAP: Structural Integrity Assessment Procedures for European Industry. Final Procedure, *Brite-Euram Project No BE95-1426* – Rotherham: British Steel.
14. **Yang S., Chao Y. J., Sutton M. A.** (1993), Higher Order Asymptotic Crack Tip in a Powe –Law Hadening Material, *Engineering Fracture Mechanics*, Vol. 45, No. 1, 99. 1 – 20.
15. **Chao Y. J., Zhu X. K., Kim Y., Lar P. S., Pechersky M. J., Morgan M. J.** (2004), Characterization of Crack-Tip Field and Constraint for Bending Specimens under Large-Scale Yielding, *International Journal of Fracture*, 127, 2004, 283-302.

Acknowledgments: The support of the Faculty of Mechatronics and Machine Design at Kielce University of Technology through scientific projects **No. 1.22/8.57 and No. 1.22/7.14** is acknowledged by the author.

Author of the paper, were involved in apprenticeship scholarships for young doctors (PhD) in the project "Capacity Development Program Educational Kielce University of Technology: training in advanced areas of technology," co-financed by the European Social Fund under the Human Capital Operational Programme, Priority IV, Activity 4.1, Sub-activity 4.1.1, no contract UDA-POKL.04.01.01-00-395/09-00; running time: 15 February 2010 - 31 December 2010.